Time-dependent Aharonov-Bohm scattering

1993 J. Phys. A: Math. Gen. 26 1749

(http://iopscience.iop.org/0305-4470/26/7/028)

J. Phys. A: Math. Gen. 26 (1993) 1749–1763. Printed in the UK

Time-dependent Aharonov–Bohm scattering

M Jursa and P Kasperkovitz

Institut für Theoretische Physik, Technische Universität Wiedner Hauptstr. 8-10, A-1040 Wien, Austria

Received 1 September 1992 , in final form 7 December 1992

Abstract. Scattering of Gaussian wavepackets by impenetrable solenoids is studied using both analytical and numerical methods. A formula for the asymptotic ($t \to \infty$) angular distribution of the scattered packet is derived and used to discuss the physical meaning of cross sections, the optical theorem, and the classical limit. Angular distributions obtained from this formula are found to be in good agreement with angular distributions calculated from numerical solutions of the Schrödinger equation.

1. Introduction

One of the differences between classical and quantum mechanics is the fact that in one case the motion of charged particles depends on the electromagnetic fields whereas in the other case it is the electromagnetic potentials that occur in the evolution equation. This difference entails striking effects, especially in multiply connected regions where the magnetic field vanishes, whereas the magnetic flux in the excluded region is different from zero. In this case the classical motion of a charged particle would be that of a free particle, except for reflections at the walls which separate the multiply connected region from the magnetic flux. In 1959 Aharonov and Bohm (AB) proposed an interference experiment [1] where an electron beam is split into two parts which pass an infinite solenoid on opposite sides and are united behind the solenoid; the intensity at this point was predicted to be a periodic function of the magnetic flux enclosed by the solenoid. To pursue their arguments AB also discussed the scattering of an electron by an impenetrable solenoid of infinite length. AB assumed the radius of the solenoid to be vanishingly small ('magnetic flux line') but it was later shown that the effect exists also for finite radius. In [1] and most of the following papers on this problem AB scattering was discussed in terms of time-independent scattering theory (TIST) as it is familiar from ordinary potential scattering.

In this paper the two-dimensional AB scattering problem is discussed in terms of time-dependent scattering theory (TDST). On a formal level this theory relates the evolution of scattered particles to that of free particles; it proves the existence of the Møller wave operators and the S-matrix, from which the scattering amplitude and the cross section can be obtained [2]. Our approach is more elementary: we study the scattering of wavepackets by impenetrable solenoids using analytical approximations and compare for a number of examples the resulting asymptotic angular distribution with that obtained from numerical integration of the time-dependent Schrödinger equation. Though calculations in TDST are more extensive than in TIST the results of

0305-4470/93/071749+15$07.50

TDST have the advantage of allowing direct interpretation according to the general rules of quantum mechanics (only square-integrable wavefunctions are considered) and of being free of apparent paradoxes (diverging cross sections). In our analytical calculations the generalized eigenfunctions calculated in TIST appear only as auxiliary mathematical objects without any physical interpretation. The usual conclusions drawn from these functions, based on the splitting into a free and a scattered wave, cover only one aspect of the problem, namely the scattering off the coil in directions that deviate from the velocity of the incoming particles. This splitting has to be avoided if one is interested in the interference pattern behind the solenoid, the phenomenon usually associated with the AB effect. Whereas different techniques are needed in TIST to describe these two aspects of the problem [3] we derive a closed formula for the asymptotic angular distribution that is valid for all directions. It is the derivation of this formula and its use in a discussion of cross sections, the optical theorem, and the classical limit, as well as the comparison with wavefunctions obtained from numerical calculations, in which this work differs from previous discussions of AB wavepacket scattering [3, 4].

In section 2 we derive a formula for the function $G^{\alpha,\rho}_{K_0,\gamma}(\varphi|+)$ whose physical meaning is the following: K_0 is the average momentum of the incoming Gaussian wavepacket and γ a parameter that measures its spatial extension. The other two parameters characterize the scatterer; α is the flux parameter and ρ is the radius of the solenoid. The quantity $|G^{\alpha,\rho}_{K_0,\gamma}(\varphi|+)|^2\,d\varphi$ gives the probability for finding the particle in the sector $(\varphi, \varphi + d\varphi)$ if a long time has elapsed since the scattering (strictly speaking this distribution is approached in the limit $t \to +\infty$).

In section 3 we use this formula to discuss the physical meaning of cross sections, the optical theorem, and the classical limit. For AB scattering the differential cross section derived from TIST is known to diverge in forward direction [1] and it has been emphasized in [2] that this should lead to experimentally observable differences between AB and ordinary potential scattering. Our analysis shows that instead of the divergence obtained for a plane wave a peak of finite height is obtained for the wavepacket. Also, outside the forward direction the difference between AB and pure potential scattering is less marked than assumed in [2]. From the expansion of the generalized eigenfunctions in partial waves the optical theorem is usually derived as a formal identity; in AB scattering both sides of this equation are of infinite magnitude [10]. We show that this form of the optical theorem can be interpreted as a balance equation only in case of pure potential scattering. The correct balance equation, formulated in section 3, shows the difference between AB and pure potential scattering more clearly: if the radius of the coil tends to zero the fraction of particles scattered off the forward direction remains finite in the AB case whereas it vanishes in case of pure potential scattering. We finally show that for increasing momentum of the incoming wavepacket (parameter K_0) the quantum aspects of the scattering, i.e. the Fraunhofer and AB interference pattern, become more and more concentrated in a narrow sector in forward direction. Outside a sector of *fixed* width one therefore finds in the classical limit ($K_0 \to \infty$) nothing but the smooth intensity as it is obtained from the classical reflection at the surface of the cylinder.

In section 4 examples of angular distributions are given for various flux parameters and diameters of the impenetrable solenoid as functions of the variable $\varphi/\pi \in [-1, +1]$. These distributions are compared to the corresponding functions obtained from numerical integration of the time-dependent Schrödinger equation. Good agreement between analytical and numerical results is found which justifies the

approximations used in section 2 and section 3.

In section 5 we finally summarize our results and the conclusions drawn from the examples (figures 1 to 5).

2. Asymptotic angular distributions

We consider wavepackets of the form

$$\psi^{\alpha,\rho}_{K_0,\gamma}(\boldsymbol{x};t)=\frac{1}{2\pi}\int_{\mathcal{R}^2}\mathrm{d}^2k\;\tilde{\psi}_{K_0,\gamma}(\boldsymbol{k})\,\chi_{\alpha,\rho}(\boldsymbol{k};\boldsymbol{x})\,\exp\left\{-\mathrm{i}\frac{\boldsymbol{k}^2}{2}t\right\} \tag{1}$$

where polar coordinates are used for the two-dimensionsnal vectors ($\boldsymbol{x}\leftrightarrow(R,\varphi)$, $\boldsymbol{k}\leftrightarrow(K,\phi)$). In (1) the function

$$\chi_{\alpha,\rho}(\boldsymbol{k};\boldsymbol{x})=\sum_m c^{\alpha}_m(\phi)\,u_{|m+\alpha|,\rho}(KR)\,\mathrm{e}^{\mathrm{i}m\varphi} \tag{2}$$

with yet undetermined coefficients $c^{\alpha}_m(\phi)$ and radial functions

$$u_{|m+\alpha|,\rho}(KR)=H_{|m+\alpha|}(KR)^*-\exp\left\{-2\mathrm{i}\Gamma_{|m+\alpha|}(K\rho)\right\}\;H_{|m+\alpha|}(KR) \tag{3}$$

is a generalized eigenfunction of the Hamiltonian

$$H=\tfrac{1}{2}(\boldsymbol{p}-\boldsymbol{A})^2 \qquad \boldsymbol{A}=-\frac{\alpha}{R}\boldsymbol{n}_{\varphi} \tag{4}$$

($m=1$, $e/c=1$, $\hbar=1$) subject to the boundary condition $u_{|m+\alpha|,\rho}(K\rho)=0$.

$$\Gamma_{|m+\alpha|}(K\rho)=\arg H_{|m+\alpha|}(K\rho) \tag{5}$$

This boundary condition follows from the assumption that the particle is reflected at the surface of the cylinder $C_\rho=\{\boldsymbol{x}\mid R\leqslant\rho\}$. This cylinder contains a solenoid enclosing a magnetic flux of magnitude $2\pi\alpha$ as can be seen from (4). The scatterer is therefore characterized by the two parameters α and ρ; for $\alpha=\rho=0$ (1) represents a free wavepacket. Note that the Hankel functions in (3) and (5) are those with asymptotic form

$$H_\nu(z)\sim\left(\frac{2}{\pi z}\right)^{1/2}\exp\left\{\mathrm{i}\left(z-\nu\frac{\pi}{2}-\frac{\pi}{4}\right)\right\}\,. \tag{6}$$

If the weight function in (1) is chosen as

$$\begin{aligned}\tilde{\psi}_{K_0,\gamma}(\boldsymbol{k})&=(2\pi\gamma)^{-1/2}\exp\left\{-\frac{1}{4\gamma}(\boldsymbol{k}-K_0\boldsymbol{n}_x)^2\right\}\\&=(2\pi\gamma)^{-1/2}\exp\left\{-\frac{1}{4\gamma}(K^2+K_0^2)\right\}\sum_M I_M(KK_0/2\gamma)\,\mathrm{e}^{\mathrm{i}M\phi}\end{aligned} \tag{7}$$

the integral (1) can be calculated analytically for $\alpha = \rho = 0$ ([6, p 223]). If

$$0 < \kappa = \frac{\sqrt{2\gamma}}{K_0} \ll 1 \tag{8}$$

one can use an asymptotic approximation for the modified Bessel functions I_M [7],

$$I_M(z) \sim (2\pi z)^{-1/2} \exp\left\{z - \frac{M^2}{2z}\right\} , \tag{9}$$

to obtain a factorization of the weight function which is more convenient for the scattering problem ($\alpha \neq 0$ and/or $\rho \neq 0$).

$$\tilde{\psi}_{K_0,\gamma}(k) = \left(2\pi\gamma K^2\right)^{-1/4} \exp\left\{-\frac{1}{4\gamma}(K - K_0)^2\right\} G_\kappa(\phi) \tag{10}$$

$$\begin{aligned} G_\kappa(\phi) &= \left(\frac{\kappa^2}{4\pi^3}\right)^{1/4} \sum_M \exp\left\{-\tfrac{1}{2}\kappa^2 M^2 + \mathrm{i}M\phi\right\} \\ &\approx \left(\pi\kappa^2\right)^{-1/4} \exp\left[-\tfrac{1}{2}(\phi/\kappa)^2\right] \qquad \text{for} \quad |\phi| \ll \pi \end{aligned} \tag{11}$$

Inserting (10) and (2) in (1) one then arrives at a double series containing the coefficients

$$c^{\alpha}_{M,m} = \frac{1}{2\pi}\int_{-\pi}^{+\pi} \mathrm{d}\phi\, \mathrm{e}^{\mathrm{i}M\phi}\, c^{\alpha}_m(\phi) . \tag{12}$$

Because of (8) and the exponential $\exp\{-\kappa^2 M^2/2\}$ contributions of terms with $|M| \gg M_0 = [1/\kappa]$ are negligible. (Here and in the following

$$\mathcal{Z} \ni [x] = x - \bar{x} \qquad 0 \leqslant \bar{x} < 1 \tag{13}$$

i.e. $[x]$ is the integer part of x). Let us assume that

$$c^{\alpha}_{M,m} = 0 \qquad \text{for} \quad M - m \neq n(\alpha) \tag{14}$$

leaving the specification of the integer function $n(\alpha)$ for later considerations. If this condition is satisfied the double series can be approximated by a finite sum; this fact makes it possible to calculate the wavefunction $\psi^{\alpha,\rho}_{K_0,\gamma}(x;t)$ at at all positions x that are sufficiently far away from the scatterer.

If the wavefunction is considered only in regions where $K_0 R \gg |M_0 - n(\alpha)|$, we can use the asymptotic form (6) of the Hankel functions in (1). Although this substitution is not justified in the terms with $|m| > |M_0 - n(\alpha)|$, this does not influence the result essentially since these terms can be neglected in any case. Extending the integration over K to the whole real line, which is justified because of the sharp peak of (10) at $K = K_0$, we arrive at the asymptotic wavefunction

$$\psi^{\alpha,\rho}_{K_0,\gamma}(R,\varphi;t) \sim \sum_{\sigma=\pm} F_{K_0,\gamma}(R,t\,|\,\sigma)\, G^{\alpha,\rho}_{K_0,\gamma}(\varphi\,|\,\sigma) \tag{15}$$

where the two radial functions are given by

$$\begin{aligned} F_{K_0,\gamma}(R,t\,|\pm) &= (8\pi^3\gamma R^2)^{-1/4}\int_{-\infty}^{+\infty} \mathrm{d}K\, \exp\Big\{-\frac{1}{4\gamma}(K-K_0)^2 \\ &\quad -\mathrm{i}\frac{K^2}{2}t \pm \mathrm{i}\Big(KR-\frac{\pi}{4}\Big)\Big\} \\ &= \Big(\frac{2\gamma}{\pi}\Big)^{1/4}[R(1-2\mathrm{i}\gamma t)]^{-1/2} \\ &\quad \times \exp\Big\{\frac{(K_0 \pm 2\mathrm{i}\gamma R)^2}{4\gamma(1-2\mathrm{i}\gamma t)} - \frac{K_0^2}{4\gamma} \mp \mathrm{i}\frac{\pi}{4}\Big\}. \end{aligned} \tag{16}$$

The real part of the exponentials in (16) is $-\gamma(1+4\gamma^2t^2)^{-1}(R \mp K_0t)^2$; accordingly in the distant past ($t \to -\infty$) the wavefunction $\psi^{\alpha,\rho}_{K_0,\gamma}(\boldsymbol{x};t)$ is given by $F_{K_0,\gamma}(R,t\,|-)\,G^{\alpha,\rho}_{K_0,\gamma}(\varphi\,|-)$, whereas it approaches $F_{K_0,\gamma}(R,t\,|+)\,G^{\alpha,\rho}_{K_0,\gamma}(\varphi\,|+)$ for $t \to +\infty$. Both these wavefunctions are asymptotic forms of free wavepackets, the one incoming and contracting in the radial direction ($\sigma = -$), the other outgoing and spreading ($\sigma = +$).

The radial distribution of the incoming wavepacket is given by

$$\begin{aligned} G^{\alpha,\rho}_{K_0,\gamma}(\varphi\,|-) &= (4\kappa^2/\pi^3)^{1/4}\,\mathrm{e}^{-\mathrm{i}n(\alpha)\varphi} \\ &\quad \times \sum_M \exp\{-\tfrac{1}{2}\kappa^2M^2 + \mathrm{i}(|M-n(\alpha)+\alpha|\,\tfrac{1}{2}\pi + M\varphi)\}\; c_{M,M-n(\alpha)}. \end{aligned} \tag{17}$$

To describe a particle that approaches the scatterer from the negative x-axis the function (17) should be centred at $\varphi = \pi$. This is achieved by choosing

$$c_{M,M-n(\alpha)} = \tfrac{1}{2}\exp\{-\mathrm{i}(|M-n(\alpha)+\alpha|\,\tfrac{1}{2}\pi + M\pi)\} \tag{18}$$

which entails

$$G^{\alpha,\rho}_{K_0,\gamma}(\varphi\,|-) = \mathrm{e}^{-\mathrm{i}n(\alpha)\varphi}\; G_\kappa(\varphi-\pi)\,. \tag{19}$$

In the distant past all wavepackets with $G^{\alpha,\rho}_{K_0,\gamma}(\varphi\,|-)$ given by (19) are localized in a narrow sector around $\varphi = \pi$ whose width is determined by κ. Convention (18) therefore guarantees the desired behaviour of the incoming wavepacket no matter how the integer $n(\alpha)$ is chosen. The physical meaning of this quantity can be seen from the expectation value of the kinematical angular momentum $\hat{L}_z^{\mathrm{kin}} = -\mathrm{i}\partial/\partial\varphi + \alpha$ for the incoming wave packet

$$\langle \hat{L}_z^{\mathrm{kin}}\rangle \to \alpha - n(\alpha) \qquad \text{for} \qquad t \to -\infty \tag{20}$$

Whereas the initial motion is parallel to the x-axis in all cases the distance of the center of the packet from the x-axis varies with $n(\alpha)$; this influences the details of the scattering process ($t \approx 0$) and shows up in the asymptotic angular distribution of

the scattered wavepacket ($t \to +\infty$). To minimize the distance $\langle \hat{L}_z^{\text{kin}} \rangle / K_0$, i.e. to make the collision as central as possible, we set

$$n(\alpha) = [\alpha] \,. \tag{21}$$

From this convention follow the relations

$$\chi_{\alpha+1,\,\rho}(k;x) = \mathrm{e}^{-\mathrm{i}\varphi}\, \chi_{\alpha,\,\rho}(k;x) \tag{22}$$

$$\psi^{\alpha+1,\rho}_{K_0,\gamma}(x;t) = \mathrm{e}^{-\mathrm{i}\varphi}\, \psi^{\alpha,\rho}_{K_0,\gamma}(x;t) \tag{23}$$

whence it is sufficient to study the wavefunctions for $0 \leqslant \alpha \leqslant 1$.

Because of

$$\int_0^\infty \mathrm{d}R\, \left|F_{K_0,\gamma}(R,t\,|\pm)\right|^2 = 1 \tag{24}$$

and [7]

$$\int_{-\pi}^{+\pi} \mathrm{d}\varphi\, \left|G^{\alpha,\rho}_{K_0,\gamma}(\varphi\,|\pm)\right|^2 = N_\kappa \tag{25}$$

$$1 - \frac{\kappa}{\sqrt{\pi}} < N_\kappa = \frac{\kappa}{\sqrt{\pi}} \sum_M \exp\{-\kappa^2 M^2\} < 1 + \frac{\kappa^2}{2\pi e} \tag{26}$$

the probability of finding the particle in a sector $\{\varphi\,|\,\varphi' < \varphi < \varphi''\}$ approaches time-independent limits for $t \to \pm\infty$. This is the equivalent of the Scattering-into-Cones-Theorem of potential scattering in three dimensions [8, 9]. At asymptotic times ($|t| \gg 1/2\gamma$) this probability is therefore well approximated by

$$\lim_{\sigma t \to \infty} \int_0^\infty \mathrm{d}R\, R \int_{\varphi'}^{\varphi''} \mathrm{d}\varphi\, \left|\psi^{\alpha,\rho}_{K_0,\gamma}(x;t)\right|^2 = \int_{\varphi'}^{\varphi''} \mathrm{d}\varphi\, \left|G^{\alpha,\rho}_{K_0,\gamma}(\varphi\,|\,\sigma)\right|^2 . \tag{27}$$

While the asymptotic angular distribution of the incoming wave packet is given by the square modulus of (19) that of the scattered wavepacket is given by the square modulus of the function

$$G^{\alpha,\rho}_{K_0,\gamma}(\varphi\,|+) = -\left(\kappa^2/4\pi^3\right)^{1/4}\, \mathrm{e}^{-\mathrm{i}[\alpha]\varphi} \times \sum_M \exp\{-\tfrac{1}{2}\kappa^2 M^2 - \mathrm{i}(|M+\bar{\alpha}|\pi + 2\Gamma_{|M+\bar{\alpha}|}(K_0\rho) - M(\varphi-\pi))\}. \tag{28}$$

Equations (27), (19), (11) and (28), constitute the main result of this paper. They show how a Gaussian wavepacket, initially moving with uniform velocity along the negative x-axis and approaching an inpenetrable solenoid at the origin, is changed by the scattering process. It should be noted that the final angular distribution (28) holds for all values of α and all directions. This makes the difference to previous treatmentments of the problem [1, 3] where part of the analytical results were obtained for special values of α only and, both in TIST and TDST, different techniques were used to obtain the intensity of the scattered wave in forward and non-forward directions. Since (28) covers the whole range of directions it is especially suited to discuss problems related to the interpretation of cross sections and the optcal theorem.

3. Cross sections, optical theorem, and classical limit

Before showing examples of angular distributions let us indicate how our results are related to TIST. The time-independent object of TDST is the scattering operator $\hat{S}$ which transforms, at an arbitrary instant t, a free wavepacket $\psi_-(x;t)$ that coincides with an interacting packet $\psi^{\alpha,\rho}(x;t)$ at $t=-\infty$, into a free packet $\psi_+(x;t)$ coinciding with the interacting packet at $t=+\infty$. For the asymptotically free wavepackets considered here this implies for $t\to+\infty$

$$\hat{S}\,F_{K_0,\gamma}(R,t\,|+)\,\mathrm{e}^{-\mathrm{i}[\alpha]\varphi}\,G_\kappa(\varphi)\sim F_{K_0,\gamma}(R,t\,|+)\,G^{\alpha,\rho}_{K_0,\gamma}(\varphi\,|+)\,. \tag{29}$$

For it is easily verified that a wavepacket, which in the distant past is of the form $F_{K_0,\gamma}(R,t\,|-)\,\mathrm{e}^{-\mathrm{i}n(\alpha)\varphi}\,G_\kappa(\varphi-\pi)$ (cf (19)), is transformed under the free evolution ($\alpha=\rho=0$) into $F_{K_0,\gamma}(R,t\,|+)\,\mathrm{e}^{-\mathrm{i}n(\alpha)\varphi}\,G_\kappa(\varphi)$ as t tends to $+\infty$. The scattering amplitude, the central object of TIST, is related to the operator $\hat{S}-\hat{1}$ [2, 9]. Restricting the discussion to large positive times we have

$$(\hat{S}-\hat{1})\,\mathrm{e}^{-\mathrm{i}[\alpha]\varphi}\,G_\kappa(\varphi)=\bar{G}^{\alpha,\rho}_{K_0,\gamma}(\varphi) \tag{30}$$

$$\bar{G}^{\alpha,\rho}_{K_0,\gamma}(\varphi)=G^{\alpha,\rho}_{K_0,\gamma}(\varphi\,|+)-\mathrm{e}^{-\mathrm{i}[\alpha]\varphi}\,G_\kappa(\varphi) \tag{31}$$

$$=\mathrm{e}^{-\mathrm{i}[\alpha]\varphi}\int_{-\pi}^{+\pi}\mathrm{d}\varphi'\,G_\kappa(\varphi-\varphi')\,g^{\bar{\alpha},K_0\rho}(\varphi') \tag{32}$$

with

$$g^{\bar{\alpha},K_0\rho}(\varphi)=\frac{1}{2\pi}\sum_M g_M^{\bar{\alpha},K_0\rho}\,\mathrm{e}^{\mathrm{i}M\varphi}$$

$$g_M^{\bar{\alpha},K_0\rho}=-\exp\left\{-\mathrm{i}(|M+\bar{\alpha}|-M)\,\pi-2\mathrm{i}\Gamma_{|M+\bar{\alpha}|}(K_0\rho)\right\}-1. \tag{33}$$

Function (33), multiplied with a factor $(1-\mathrm{i})\sqrt{\pi/K_0}$, is nothing but the scattering amplitude as it is derived in TIST from the asymptotic form of the generalized eigenfunctions [5, 3, 11] (here $\chi(K_0\boldsymbol{n}_x;\boldsymbol{x})$ for $R\to\infty$, $0<\varphi<2\pi$).

Since $G_\kappa(\varphi)\approx 0$ for $1.2\kappa<|\varphi|\leqslant\pi$ the probability of finding the particle in a certain direction outside the forward sector $|\varphi|<1.2\kappa$ becomes proportional to the square modulus of (30). As (32) shows this function is obtained from the scattering amplitude by smoothing with the bell-shaped function (11). As the width of this function decreases with increasing diameter of the incoming wavepacket (K_0 fixed, $\gamma\to 0$) the differential cross section of TIST corresponds to the asymptotic angular distribution of extended wavepackets. If γ, and hence κ, is so small that $g^{\bar{\alpha},K_0\rho}(\varphi')$ varies within the interval $\varphi-1.2\kappa<\varphi'<\varphi+1.2\kappa$ only by a small amount then

$$\bar{G}^{\alpha,\rho}_{K_0,\gamma}(\varphi)\approx(4\pi\kappa^2)^{1/4}\,g^{\bar{\alpha},K_0\rho}(\varphi) \tag{34}$$

and

$$|\bar{G}^{\alpha,\rho}_{K_0,\gamma}(\varphi)|^2\approx\frac{\kappa}{\sqrt{\pi}}\left|\sum_M g_M^{\bar{\alpha},K_0\rho}\,\mathrm{e}^{\mathrm{i}M\varphi}\right|^2. \tag{35}$$

Up to a factor $\sqrt{\pi}/\kappa K_0$ the RHS of (35) coincides with the differential cross section derived in TIST for a solenoid of radius ρ [2, 5]. In the limit $\rho \to 0$ this function approaches the cross section of AB, since (33) becomes proportional to the series representation of the AB scattering amplitude in this limit [2, 5, 3]; for $0 < \varphi < 2\pi$ this series can be summed [11, 2] which results in the closed expression of AB [1].

The proportionality factor that relates the probability density $|G^{\alpha,\rho}_{K_0,\gamma}(\varphi|+)|^2$ to the differential cross section results from the different normalization of the two quantities; this will be discussed in more detail in the following. Here we want to emphasize that this proportionality holds only for $\kappa \ll 1$ and and only outside the forward sector. Since the function (33) diverges as $(\sin\pi\bar{\alpha})/\varepsilon$ for $\varepsilon = |\varphi| \to +0$ [1, 11], (35) is not valid near $\varphi = 0$. From the divergence of the scattering amplitude at this point it was concluded that for $0 < \bar{\alpha} < 1$ both the differential cross section in the forward direction and the total cross section diverge [2, 12], as if this were a strange physical phenomena. However, these propositions merely show that care has to be taken in interpreting results derived in TIST. On the other hand, the observable consequences of the singularity of (33) are easily understood within TDST. No problems occur in the forward direction for two reasons. (i) It is not the scattering amplitude itself that enters in the asymptotic angular distribution but its smoothed form (32) which is bounded everywhere. The smoothing is a consequence of the spreading of initial momenta (see (1),(10),(11)) which is unavoidable for normalizable states. (ii) The angular distribution in the forward sector is not only determined by the smoothed scattering amplitude (32) but also by the distribution of the free wavepacket and the interference of these two functions (see (27),(31)). All that can be concluded from the divergence of (33) at $\varphi = 0$ is that high intensities are to be expected near the boundaries of the forward sector ($\varphi = \pm 1.2\kappa$), especially for $\bar{\alpha} = 1/2$.

The initial data should also be taken into account in the interpretation of the total cross section and the optical theorem. Conservation of norm gives

$$N_\kappa = \int_{-\pi}^{+\pi} \mathrm{d}\varphi\, |\mathrm{e}^{-\mathrm{i}[\alpha]\varphi}\, G_\kappa(\varphi) - \bar{G}^{\alpha,\rho}_{K_0,\gamma}(\varphi)|^2 = N_\kappa + 2\mathrm{Re}\int_{-\pi}^{+\pi} \mathrm{d}\varphi\, \mathrm{e}^{\mathrm{i}[\alpha]\varphi} G_\kappa(\varphi)^* \bar{G}^{\alpha,\rho}_{K_0,\gamma}(\varphi) + \int_{-\pi}^{+\pi} \mathrm{d}\varphi\, |\bar{G}^{\alpha,\rho}_{K_0,\gamma}(\varphi)|^2 \quad (36)$$

or

$$\frac{\kappa}{\sqrt{\pi}}(-2)\,\mathrm{Re}\sum_M \mathrm{e}^{-\kappa^2 M^2} g_M^{\bar{\alpha},K_0\rho} = \frac{\kappa}{\sqrt{\pi}}\sum_M \mathrm{e}^{-\kappa^2 M^2} |g_M^{\bar{\alpha},K_0\rho}|^2. \quad (37)$$

The RHS of (37) is obviously positive and vanishes only for $\alpha = \rho = 0$; for a scattering process both sides are therefore positive. Each side is also bounded from above by $4 + 2\kappa^2/\pi e$ as follows from $|g_M^{\bar{\alpha},K_0\rho}| < 2$ and (26). Equation (37) holds for all $\kappa > 0$, the number of terms that have to be considered being of the order $M_0 = [1/\kappa]$. How many of these terms contribute essentially to the sums depends on the flux parameter $\bar{\alpha}$ because $\Gamma_{|M+\bar{\alpha}|}(K_0\rho) \to -\pi/2$ and hence

$$|g_M^{\bar{\alpha},K_0\rho}| \to 2(\sin\bar{\alpha}\pi) \qquad \text{for} \qquad |M| \to \infty\,. \quad (38)$$

For pure potential scattering ($\bar{\alpha} = 0$) the series essentially reduce to finite sums and both sides of (37) vanish as κ in the limit $\kappa \to 0$. If both sides are divided by κ before

the limit is taken one arrives at the familiar optical theorem which relates the value of the scattering amplitude in forward direction to the average of its square modulus, i.e. to the total cross section σ_T. For $0 < \bar{\alpha} < 1$ the situation is quite different: the sums diverge as κ^{-1} and both sides of (37) tend to $4(\sin \bar{\alpha}\pi)^2$ in the limit $\kappa \to 0$. In this case division by κ prior to the limit $\kappa \to 0$ results in an optical theorem that is formally identical to the usual one [10]; but this equation relates two quantities which, being of infinite magnitude, do not admit any direct physical interpretation.

In TIST the optical theorem is interpreted as a balance equation: the side proportional to the scattering amplitude at position $\varphi = 0$ is interpreted as the 'loss' of particles in forward direction while the other side, the total cross section σ_T, is considered as 'gain' of particles in the other directions. To interpret (37), or a limiting form thereof, in this way calls for additional arguments since the quantities on both sides are related to the function $\bar{G}^{\alpha,\rho}_{K_0,\gamma}(\varphi)$ which, contrary to the functions $G^{\alpha,\rho}_{K_0,\gamma}(\varphi|\pm)$, does not have a probabilistic meaning. Of course (37) is mathematically equivalent to the conservation law (36); but to obtain a true balance equation one has to subtract from both sides the quantity

$$R_\kappa(c) = \int_{-c\kappa}^{+c\kappa} \mathrm{d}\varphi \, |\bar{G}^{\alpha,\rho}_{K_0,\gamma}(\varphi)|^2 \tag{39}$$

where the constant c is chosen such that $|G_\kappa(c\kappa)|$ is smaller than a given error bound (eg $c = 1.2$). Because of (31) the RHS of the new equation then represents the probability of finding the particle finally outside the forward sector $|\varphi| < c\kappa$; accordingly the LHS gives the probability that the particle is removed from the forward direction by the scattering process. This probability depends on the characteristics of both the incoming wavepacket (K_0, γ) and the scatterer (α, ρ), and on the definition of the forward sector (c). To which limit this probability tends in the 'plane wave limit' $\kappa \to 0$ (K_0 fixed, $\gamma \to 0$) depends crucially on the flux parameter α.

For pure potential scattering ($\bar{\alpha} = 0$) the scattering amplitude (33) is a continuous function. If κ is sufficiently small smoothing with G_κ therefore gives (34). The correction term (39) is then of order κ^2 and adds only a small correction to the RHS of (37) which is $O(\kappa)$. The probability that the particle is scattered by the impenetrable cylinder then becomes $\kappa K_0 \sigma_T/\sqrt{\pi}$. That this probability vanishes in the limit $\kappa \to 0$, whereas σ_T remains finite, is a result of different normalizations: in TIST the total cross section σ_T is normalized by the flux of the 'incoming' plane wave; in TDST the wave function is normalized to one whence the probability that the incoming particle 'hits' the obstacle ($|M| < K_0\rho$) is equal to $2K_0\rho\kappa/\sqrt{\pi}$ for $\kappa \ll 1$. Because of the short range of the interaction it is therefore legitimate to interpret the optical theorem of TIST as balance equation provided that both sides of this equation are multiplied with $\kappa K_0/\sqrt{\pi}$.

To see what happens in case of non-integer α it is convenient to split the asymptotic wavefunction into a pure AB wave function and a remainder

$$G^{\alpha,\rho}_{K_0,\gamma}(\varphi|+) = G^{\alpha,0}_{K_0,\gamma}(\varphi|+) + \bar{G}^{\alpha,\rho}_{K_0,\gamma}(\varphi). \tag{40}$$

Like the function $\bar{G}^{\alpha,\rho}_{K_0,\gamma}(\varphi)$ in potential scattering the remainder term in (40) is essentially a finite sum that becomes a continuous function proportional to $\kappa^{1/2}$ if $\kappa \ll 1$. The pure AB term is given by (28) with $\Gamma_{|M+\bar{\alpha}|}(K_0\rho) = -\pi/2$. For small

κ *the sum may be approximated by an integral which can be evaluated analytically* ([13, p 451]). The result is

$$G^{\alpha,0}_{K_0,\gamma}(\varphi|+) \approx \mathrm{e}^{-\mathrm{i}[\alpha]\varphi}\ (\pi\kappa^2)^{-1/4} \times \exp\left\{-\frac{1}{2}(\varphi/\kappa)^2\right\}\left((\cos\bar{\alpha}\pi) + (\sin\bar{\alpha}\pi)(-\mathrm{i})\,\mathrm{erf}\,\frac{\mathrm{i}}{\sqrt{2}}(\varphi/\kappa)\right). \quad (41)$$

Note that $f(x) = -\mathrm{i}\,\mathrm{erf}(\mathrm{i}x/\sqrt{2}) = f(x)^* = -f(-x)$ so that $G^{\alpha,\rho}_{K_0,\gamma}(0) = 0$ for $\bar{\alpha} = 1/2$. As κ tends to zero, the loss and gain terms for pure AB scattering then approach finite values whose magnitude depends only on the definition of the forward sector:

$$1 - \int_{-c\kappa}^{+c\kappa} \mathrm{d}\varphi\, |G^{\alpha,0}_{K_0,\gamma}(\varphi|+)|^2 = (\cos\bar{\alpha}\pi)^2\, X(c) + (\sin\bar{\alpha}\pi)^2\, Y(c) \quad (42)$$

$$X(c) = \frac{2}{\sqrt{\pi}}\int_c^\infty \mathrm{d}x\ \mathrm{e}^{-x^2} \quad = \quad \mathrm{erfc}\,c$$
$$Y(c) = \frac{2}{\sqrt{\pi}}\int_c^\infty \mathrm{d}x\ \mathrm{e}^{-x^2}\left(\mathrm{erf}\,\frac{\mathrm{i}}{\sqrt{2}}x\right)^2 \quad (43)$$

To obtain (43) from (41) we made use of the relations $X(0) = Y(0) = 1$ (see [6, p 123]) which are consistent with the normalization of $G^{\alpha,0}_{K_0,\gamma}(\varphi|+)$. Equation (43) shows that for $0 < \bar{\alpha} < 1$ there is always a finite probability of the particle being scattered, no matter how the forward sector is defined in detail or how far extended the incoming wavepacket is in the beginning. This holds also for a solenoid of finite diameter since the remainder term in (41) gives only corrections of order $\kappa^{1/2}$ in the balance equation. This qualitative difference to short-range potential scattering may be attributed to the long range of the electromagnetic interaction which shows up in the slow decay of the vector potential (4).

The limit $\kappa \to 0$ may also be considered as classical limit $K_0 \to \infty$, γ fixed, provided that this limit is also taken into account in the remainder term $\tilde{G}^{\alpha,\rho}_{K_0,\gamma}(\varphi)$. If the extension of the free wave packet at $t = 0$ is much larger than the diameter of the solenoid, ie if $1/\sqrt{2\gamma} \gg \rho$, then the remainder term may be approximated by

$$\tilde{G}^{\alpha,\rho}_{K_0,\gamma}(\varphi) \approx {}^{S}\tilde{G}^{\alpha,\rho}_{K_0,\gamma}(\varphi) + {}^{R}\tilde{G}^{\alpha,\rho}_{K_0,\gamma}(\varphi) \quad (44)$$

where

$${}^{S}\tilde{G}^{\alpha,\rho}_{K_0,\gamma}(\varphi) = -\left(\frac{\gamma}{2\pi^2 K_0^2}\right)^{1/4}\left\{S([K_0\rho+1],\varphi)\,\mathrm{e}^{-\mathrm{i}\bar{\alpha}\pi+\mathrm{i}[K_0\rho]\varphi/2} + S([K_0\rho],\varphi)\,\mathrm{e}^{\mathrm{i}\bar{\alpha}\pi-\mathrm{i}[K_0\rho+1]\varphi/2}\right\} \quad (45)$$
$$S(N,\varphi) = \frac{\sin(N\varphi/2)}{\sin(\varphi/2)}$$

is the 'shadow' contribution and

$${}^{R}\tilde{G}^{\alpha,\rho}_{K_0,\gamma}(\varphi)\left(\frac{\gamma\rho^2}{2\pi}\right)^{1/4}\left(\sin\frac{\varphi}{2}\right)^{1/2} \times \exp\left\{-2\mathrm{i}K_0\rho\sin\frac{\varphi}{2} - \mathrm{i}\frac{3\pi}{4} - \mathrm{i}\alpha(\varphi-\pi)\right\} \quad (46)$$

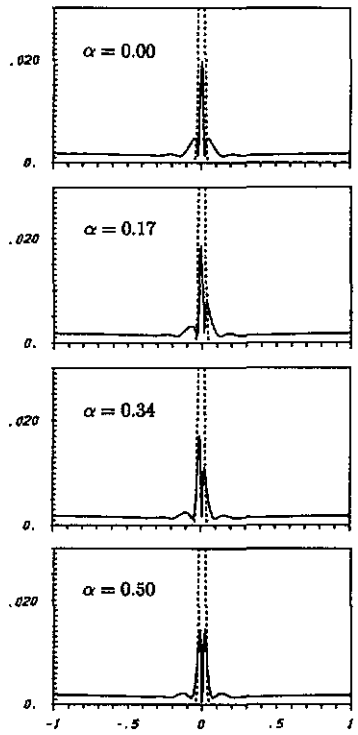

Figure 1. Asymptotic angular distribution of scattered wavepackets obtained by analytical approximations (density of probability (27) as function of the dimensionless variable φ/π, observation at time $t \to \infty$). Start parameters $\gamma = 1.54$, $K_0 = 30$; full curves $\rho = 0.20$ (thick coil), $0 \leqslant \alpha \leqslant 0.5$; broken curve $\rho = 0$, $\alpha = 0$ (free motion).

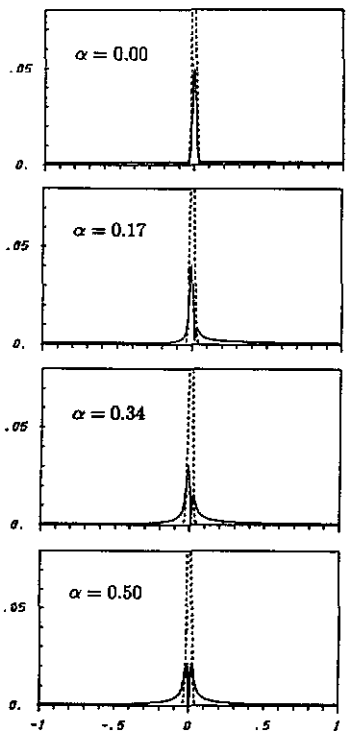

Figure 2. Asymptotic angular distribution of scattered wavepackets obtained by analytical approximations. Start parameters $\gamma = 1.54$, $K_0 = 30$; full curves $\rho = 0.01$ (thin coil), $0 \leqslant \alpha \leqslant 0.5$; broken curve $\rho = 0$, $\alpha = 0$ (free motion).

is the 'reflection' contribution ($0 < \varphi < 2\pi$). Approximation (44) is obtained by truncating the series at $M = \pm[K_0\rho]$; the shadow part (45) is then summable while the reflection part can be approximated by an integral which is calculated by the method of stationary phase (cf [14] for $\bar{\alpha} = 0$). For large K_0 both the pure AB contribution (41) and the shadow contribution (45) decay rapidly outside narrow sectors of order K_0^{-1} which contain the forward direction $\varphi = 0$. In the classical limit the probability of finding the particle outside a forward sector of given width 2ε is therefore given by the reflection contribution (46), ie

$$\int_{\varepsilon}^{2\pi-\varepsilon} \mathrm{d}\varphi \, |G^{\alpha,\rho}_{K_0,\gamma}(\varphi|+)|^2 \to \sqrt{2\gamma/\pi}\,\sigma_G + \mathrm{O}(\varepsilon^2) \qquad \text{for} \quad K_0 \to \infty. \tag{47}$$

In (47) $\sigma_G = 2\rho$ is the geometrical cross section and the leading term is nothing but the probability that the incoming particle hits the coil. The dependence on the magnetic flux is only seen in the forward sector $|\varphi| < \varepsilon$, where the form of the angular distribution depends crucially on $\bar{\alpha}$. But if the limit $\varepsilon \to 0$ is performed after the limit $K_0 \to \infty$ the simple geometrical picture of classical scattering (specular reflection at the surface of the cylinder) is obtained independently of the enclosed magnetic flux.

4. Examples

Using the well-known properties of the Hankel functions the asymptotic angular distribution $|G^{\alpha,\rho}_{K_0,\gamma}(\varphi|+)|^2$ was calculated explicitly for $\gamma = 1.54$, $K_0 = 10$, 30 and $\rho = 0.01$, 0.20. The corresponding values of κ are 0.18 and 0.06; although the first one does not satisfy the well condition $\kappa \ll 1$, which was used in the derivation of (29), this example was included for comparison with the corresponding numerical solution of the time-dependent Schrödinger equation.

The angular distributions obtained from the wavefunction (29) are shown in figures 1 to 3. To check these results we also calculated the angular distribution for wavefunctions obtained from numerical integration of the Schrödinger equation. The numerical scheme, as well as results obtained for solenoids of finite length, will be presented elsewhere; here we list only the differences between the numerical calculation and the analytical treatment of section 2. (i) In the numerical calculation the initial wavefunction was chosen to be a Gaussian wavepacket, centred at $\boldsymbol{x} = -R_0\,\boldsymbol{n}_x$ and having a central wave vector $\boldsymbol{k}_0 = K_0\,\boldsymbol{n}_x + K_1(\alpha)\,\boldsymbol{n}_y$. The value of $K_1(\alpha) = -\alpha/R_0$ was determined from the condition $\langle \hat{L}^{\rm kin}_z \rangle = 0$ (cf section 2). Such a wavepacket can be expressed in the form (1) if a Gaussian centred at $\boldsymbol{k}_0$ is used for the weight function and a plane wave for the generalized eigenfunction. The wavefunctions used in the two treatments are therefore not identical, but very similar to each other since K_0 and γ have the same meaning and $\langle \hat{L}^{\rm kin}_z \rangle$ is very small in both cases (central collisions). (ii) The evolution of the initial wavepacket was followed until the radial peak of the outgoing scattered wave packet reached the circle $R = 3R_0$. The radial distribution calculated for this wavefunction according to (27) is shown as full curve in figures 4 and 5; dashed curves show the radial distribution of the scattered wavepacket at earlier instants ($R = R_0$). These curves were included to show how these distributions change in time since the asymptotic region was not reached in the numerical calculations. In the numerical calculations the observation times were of order $3R_0/K_0$, which means $t \approx 0.9$ for $K_0 = 10$ and $t \approx 0.3$ for $K_0 = 30$; at these times the asymptotic form of the wave functions is not yet reached because (15) can be expected to hold only for times much larger than $1/2\gamma \approx 0.2$.

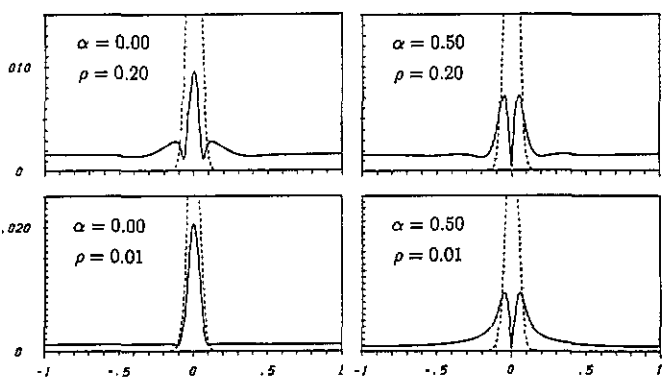

Figure 3. Asymptotic angular distribution of scattered wavepackets obtained by analytical approximations. Start parameters $\gamma = 1.54$, $K_0 = 10$; full curves $\rho = 0.01$ and 0.20, $\alpha = 0.0$ and 0.5; broken curve $\rho = 0$, $\alpha = 0$ (free motion).

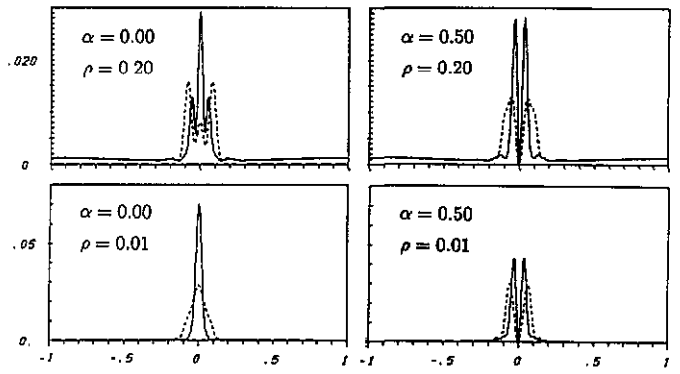

Figure 4. Angular distribution of scattered wavepackets obtained by numerical calculations, observation at time t (density of probability (27) as function of the dimensionless variable φ/π, t finite). Start parameters $\gamma = 1.54$, $K_0 = 30$; coil radii $\rho = 0.01$ and 0.20; flux parameters $\alpha = 0.0$ and 0.5. Full curve $t = 0.3$; broken curve $t = 0.1$.

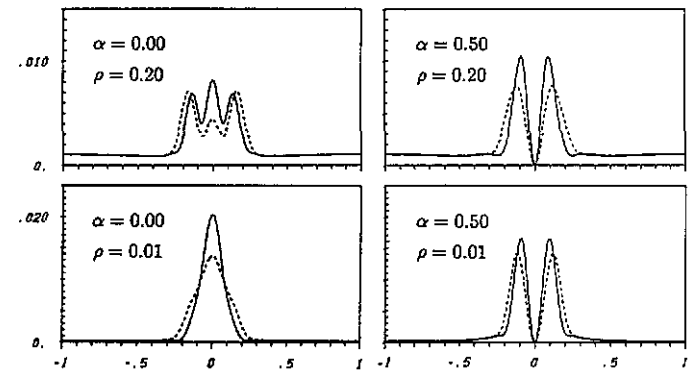

Figure 5. Angular distribution of scattered wave packets obtained by numerical calculations, observation at time t. Start parameters $\gamma = 1.54$, $K_0 = 10$; coil radii $\rho = 0.01$ and 0.20; flux parameters $\alpha = 0.0$ and 0.5. Full curve $t = 0.9$; broken curve $t = 0.3$.

The differences in the initial data and the instant of the final observation considered agreement between the analytical and the numerical angular distributions is satisfactory. In any case the following conclusions can be drawn from both calculations: (i) Outside the forward sector $|\varphi| < 1.2\kappa$, ie outside those directions where the particle would be found if there were no scattering, the angular distribution does not change very much if the magnetic flux is varied. Only for very thin coils ($\rho = 0.01$) and flux parameters near $\bar{\alpha} = 0.5$ the probability of finding the particle near (but still outside) the forward sector becomes markedly larger. This increase of the intensity near the forward direction is related to the divergence of the AB scattering amplitude at $\varphi = 0$; however, the observable consequences of this divergence are much less pronounced than conjectured by Ruisenaars [2]. (ii) Within the forward sector the intensity varies continuously with the flux parameter. As $\bar{\alpha}$ is increased from 0 to 0.5 the maxima and minima of pure potential scattering ($\bar{\alpha} = 0$)

are continuously shifted and deformed. In this variation one of the two minima adjacent to the central peak of potential scattering becomes the central minimum for $\tilde{\alpha} = 0.5$; its neighbouring maxima originate from the central and the first side maximum of potential scattering, respectively. In the height and location of maxima and minima the AB interference effect is clearly visible within the forward sector. Studying the properties of the generalized eigenfunction $\chi(K_0 n_x; x)$ in forward direction ($x = R n_x + y n_y$, $R \to \infty$) Olariu and Popescu [3] predicted a Fraunhofer-like strip pattern in this region. In a superposition of many eigenfunctions, needed for the formation of a wavepacket, these fluctuations obviously cancel each other, except for the peaks nearest to $\varphi = 0$ which are essentially the same for all wavelengths.

The transition from $K_0 = 10$ to $K_0 = 30$ with γ, ρ, and α fixed, may be considered as a first step towards the plane wave or the classical limit. The curves are seen to change in a way that is to be expected from the discussion of these limits in section 3.

5. Conclusion

In this paper the scattering of charged particles by an impenetrable solenoid of infinite length and finite diameter is reconsidered. Whereas most of the previous treatments [1, 5, 11, 12] used time-independent scattering theory (TIST) to discuss this problem we use time-dependent scattering theory (TDST). Using various analytical approximations we obtain, for wavepackets that look like free Gaussian wavepackets in the distant past ($t \to -\infty$), the form of the wavefunctions long after the scattering ($t \to +\infty$). From this the asymptotic angular distribution, i.e. the time-independent probability of finding the particle within a given sector $\varphi' < \varphi < \varphi''$, is derived. The probability density of this distribution is obtained in form of a series (see (27) and (28)) which is valid for all angles φ. It therefore includes both scattering off the coil and the Aharonov–Bohm–Fraunhofer interference pattern behind the coil. This is in contrast to previous studies of AB wavepacket scattering [3, 4] where different techniques were used to obtain the angular distribution in these two regions.

In section 3 equations (27) and (28) are used to discuss the physical meaning of the total cross section and the optical theorem. It is shown that the divergences found for non-integer flux in TIST [2, 10, 12] must not be taken as observable effects. These apparent paradoxes are resolved and a consistent description of the qualitative difference between AB and pure potential scattering is obtained if TDST is used instead of TIST. Also the classical limit is easily understood within this framework: if K_0, the average momentum of the incoming packet, is increased, while all other parameters of the problem are kept fixed, the sector behind the coil where the Aharonov–Bohm–Fraunhofer interference pattern is seen becomes more and more narrow. In the limit $K_0 \to \infty$ all quantum aspects of the scattering, including the magnetic AB effect, are concentrated in the forward direction while for all other directions the intensity of the scattered packet may be attributed to specular reflections at the surface of the solenoid.

In section 4 we finally compute explicitly for various sets of parameters the asymptotic angular distribution obtained in section 2 by analytical approximations and compare these distributions with the corresponding ones obtained by numerical integration of the time-dependent Schrödinger equation. From these functions, displayed in figures 1–5, the following can be concluded: if the solenoid is looked

at from a certain direction the probability of finding the particle after the scattering varies continuously with the enclosed flux. The effect of this variation is most clearly seen in the forward direction where the minima are shifted and the maxima deformed (see especially figures 1 and 2). Outside the forward direction the action of trapped fluxes is less pronounced and can be observed for very thin solenoids only.

Acknowledgments

This work was supported by the Austrian Science Foundation (Fonds zur Förderung der wissenschaftlichen Forschung) under project no P7888-TEC.

References

[1] Aharonov Y and Bohm D 1959 *Phys. Rev.* **115** 485
[2] Ruisenaars S N M 1983 *Ann. Phys., NY* **146** 1
[3] Olariu S and Popescu I I 1985 *Rev. Mod. Phys.* **57** 339
[4] Kretzschmar M 1965 *Z. Phys.* **185** 84
[5] Aharonov Y, Au C K, Lerner E C and Liang J Q 1984 *Phys. Rev.* D **29** 2396
[6] Prudnikov A P, Brytshkov Yu A and Maritshev O I 1983 *Integrals and Sums* vol 2 *Special Functions* (Moscow: Nauka)
[7] Kasperkovitz P 1980 *J. Math. Phys.* **21** 6
[8] Dollard J D 1969 *Commun. math. Phys.* **12** 193
[9] Amrein W O, Jauch J M and Sinha K B 1977 *Scattering Theory in Quantum Mechanics* (Reading MA: Benjamin)
[10] Gu Z Y and Qian S W 1989 *Phys. Lett.* **136A** 6
[11] Berry M V, Chambers R G, Large M D, Upstill C and Walmsley J C 1980 *Eur. J. Phys.* **1** 154
[12] Henneberger W C 1980 *Phys. Rev.* A **22** 1383
[13] Prudnikov A P, Brytshkov Yu A and Maritshev O I 1981 *Integrals and Sums* vol 1 *Elementary Functions* (Moscow: Nauka)
[14] Morse P M and Feshbach H 1953 *Methods of Theoretical Physics* pt II (New York: McGraw-Hill)